

Characterization of Random and Multiblock Copolymers of Highly Sulfonated Poly(arylene ether sulfone) for a Proton-Exchange Membrane

Cui Liang, Tatsuo Maruyama, Yoshikage Ohmukai, Tomohiro Sotani, Hideto Matsuyama

Department of Chemical Science and Engineering, Kobe University, 1-1 Rokkodai, Nada-ku, Kobe 657-8501, Japan

Received 10 January 2009; accepted 18 April 2009

DOI 10.1002/app.30658

Published online 24 June 2009 in Wiley InterScience (www.interscience.wiley.com).

ABSTRACT: Random and multiblock copolymers of sulfonated poly(arylene ether sulfone) (SPAES) were synthesized and characterized to compare the differences in the properties of proton-exchange membranes made with random and multiblock SPAES copolymers. Atomic force microscopy observations and small-angle X-ray scattering measurements suggested the presence of nanoscale, clusterlike structures in the multiblock SPAES copolymers but not in the random SPAES copolymers. Proton-exchange membranes were prepared from random and multiblock copolymers with various ion-exchange capacities (IECs). The water uptake, proton conductivity, and methanol permeability of the SPAES membranes depended on the IECs

of the random and multiblock SPAES copolymers. At the same IEC, the multiblock SPAES copolymers exhibited higher performances with respect to proton conductivity and proton/methanol permeation selectivity than the random SPAES copolymers. The higher performances of the multiblock SPAES copolymers were thought to be due to their clusterlike structure, which was similar to the ionic cluster of a Nafion membrane. © 2009 Wiley Periodicals, Inc. *J Appl Polym Sci* 114: 1793–1802, 2009

Key words: copolymerization; proton-exchange; membranes; sulfonated poly(arylene ether sulfone); multiblock copolymer

INTRODUCTION

In the last decade, the development of new power sources to solve the energy crisis has been a worldwide issue. Direct methanol fuel cells (DMFCs) are some of the most attractive power sources because of their high energy density and low environmental pollution.¹ Proton-exchange membranes (PEMs), which are sandwiched between the anodes and cathodes of cells, play an important role in the development of DMFCs.² The qualities needed for high-performance PEMs include high proton conductivity, low fuel permeability, and good thermal and mechanical stability.³ Hydrated perfluorosulfonic acid membranes such as Nafion are well-known materials for PEMs. These membranes exhibit excellent chemical, mechanical, and thermal stability in addition to high proton conductivity. However, the high methanol permeability of these membranes limits their application in the DMFC field.^{4–6} Because of this, extensive efforts have been made to develop alternative membrane materials, such as sulfonated polysulfone,⁷ sulfonated poly(arylene ether sulfone) (SPAES),⁸ sulfonated poly(aryl ether ketone),⁹ and

polybenzimidazole.¹⁰ Of these polymers, SPAES has attracted considerable attention because of its high chemical and thermal stability and excellent mechanical strength.⁸

Sulfonated polymers can be synthesized by the postsulfonation of commercial polymers or the direct copolymerization of sulfonated monomers.⁸ The direct copolymerization of sulfonated monomers with other nonsulfonated aromatic monomers is more attractive because the degree of sulfonation can be precisely controlled by the adjustment of the ratio of sulfonated monomers to nonsulfonated monomers in the polymerization.

Random and multiblock copolymers can be prepared by the direct copolymerization method. It has been reported that the composition and morphology of ionomers have a close relationship with the proton conductivity and tensile strength of membranes.¹¹ In comparison with random sulfonated polymers, in which sulfonate groups are randomly grafted onto a polymer's backbone, multiblock copolymers are more interesting because they have highly ordered sequences of both hydrophilic and hydrophobic blocks, which can easily form a microphase-separation morphology like that of Nafion.¹¹ Zhao et al.¹² reported the synthesis of a series of block sulfonated poly(ether ether ketone) (SPEEK) copolymers and compared their properties with those of random SPEEK. The results showed that block SPEEK had higher proton conductivity than

Correspondence to: H. Matsuyama (matuyama@kobe-u.ac.jp).

random SPEEK. Ishikawa et al.² synthesized multi-block copolymers of sulfonated poly(aryl ether ketone)s and reported that a multiblock copolymer showed higher proton/methanol selectivity than a random copolymer. Roy et al.¹³ studied the influence of the chemical composition and sequence length on the transport properties of PEMs and observed that under partially hydrated conditions, block copolymers showed greater proton conductivity than random copolymers. However, in most of the reports, the morphology differences between random and multiblock copolymers and the effects of the membrane morphology on the properties of the membranes are not discussed in detail.

The objectives of this study were to directly synthesize random and multiblock SPAES copolymers and to compare the membrane property differences when each of them was used as the material for a PEM. Two sulfonated monomers were introduced into the SPAES copolymers to develop the phase separation between the hydrophilic and hydrophobic parts of the copolymers. PEMs were successfully prepared from random and multiblock copolymers with various ion-exchange capacities (IEC) and morphologies. The effects of the microstructures of the copolymers on the membrane morphology, water uptake, proton conductivity, and methanol permeability of the membranes were studied.

EXPERIMENTAL

Materials

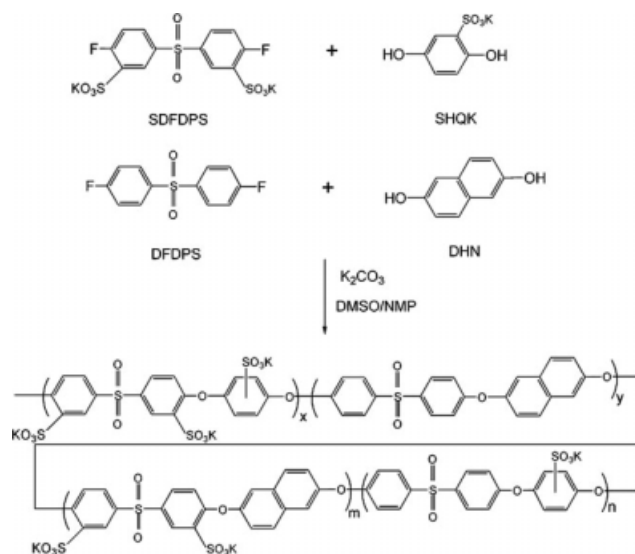
4,4'-Difluorodiphenyl sulfone (DFDPS) was purchased from Aldrich (Steinheim, Germany). Hydroquinone sulfonic acid potassium salt (SHQK), 2,6-dihydroxynaphthalene (DHN), and potassium carbonate were obtained from Wako Pure Chemical Industries (Tokyo, Japan). Dehydrated dimethyl sulfoxide (DMSO), *N*-methyl-2-pyrrolidone (NMP), and toluene were also purchased from Wako Pure Chemical Industries and used as received. Sulfonated 4,4'-difluorodiphenyl sulfone (SDFDPS) was synthesized in our laboratory with a process reported elsewhere.⁸

Nafion 117 membrane was purchased from Aldrich.

Polymerization

Synthesis of random SPAES copolymers (Scheme 1)

The synthesis of random SPAES copolymers was conducted in a three-necked flask equipped with a nitrogen inlet and a Dean–Stark trap. A typical polymerization procedure was as follows: SDFDPS (4.906 g, 10 mmol), SHQK (2.283 g, 10 mmol), DHN (3.203 g, 20 mmol), and DFDPS (5.085 g, 20 mmol) were dissolved in 60 mL of dehydrated DMSO and

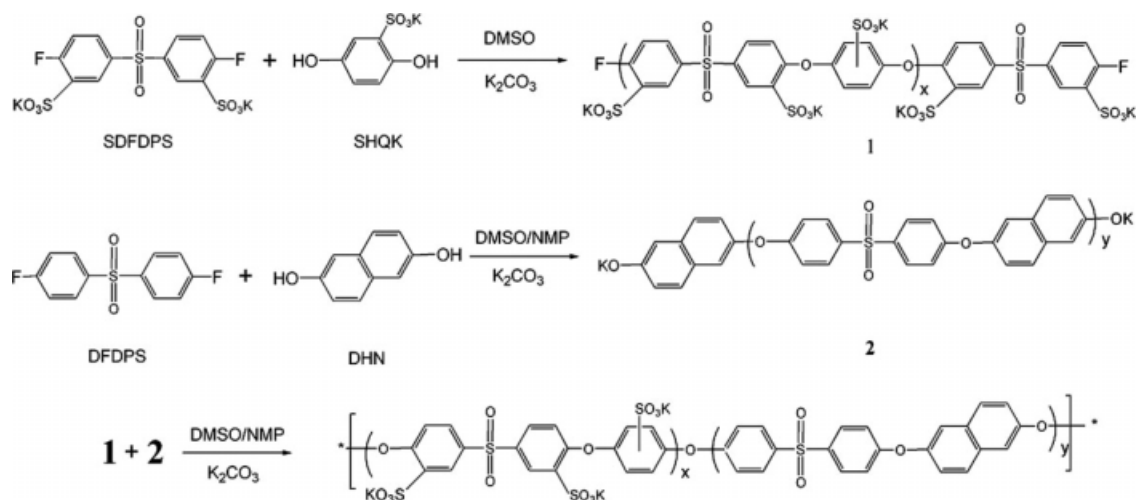


Scheme 1 Synthesis of random SPAES copolymers.

NMP (1 : 1 v/v). Toluene (10 mL) was used as an azeotropic agent. After the monomers were dissolved, potassium carbonate (6.219 g, 45 mmol) was added. Then, the pressure in the flask was reduced to 25 kPa, and the mixture was stirred at 95°C for 5 h to remove water from the reaction medium. After dehydration, the pressure was restored to atmospheric pressure, and the toluene–water mixture in the Dean–Stark trap was removed. The pressure in the flask was then reduced to 20 kPa and maintained for 1 h to remove the residual toluene in the flask. After the removal of the toluene, the pressure was again restored to atmospheric pressure, and the reaction temperature was raised to 140°C. The reaction was conducted for 24 h, and a brown, viscous polymer solution was obtained. After the reaction, the mixture was poured into a large quantity of deionized water to precipitate the synthesized polymer. The obtained polymer was then immersed in a 6 wt % HCl solution overnight to convert the polymer into an acid form. The excess acid was washed with water, and then the polymer was dried in a vacuum oven at 80°C for 24 h.

Synthesis of multiblock SPAES copolymers (Scheme 2)

Multiblock SPAES copolymers were synthesized with the method of Onodera et al.¹⁴ The typical polymerization procedure was as follows: SDFDPS (5.200 g, 10.6 mmol) and SHQK (2.283 g, 10 mmol) were dissolved in DMSO (30 mL) in a three-necked flask, which was equipped with a nitrogen inlet and a Dean–Stark trap. After the monomers were dissolved, an excess of potassium carbonate (2.073 g, 15 mmol) was added. The reaction medium was



Scheme 2 Synthesis of multiblock SPAES copolymers.

dehydrated at 25 kPa and 95°C for 5 h. After dehydration, the pressure was restored to atmospheric pressure, and the toluene–water mixture in the Dean–Stark trap was removed. Then, the pressure in the flask was reduced to 20 kPa and maintained for 1 h to remove the residual toluene in the flask. The pressure was then restored to atmospheric pressure, and the reaction was conducted at 140°C for 12 h. The resultant solution of hydrophilic oligomers was used for the subsequent block copolymerization.

For the syntheses of hydrophobic oligomers, DHN (3.364 g, 21 mmol), DFDPS (5.085 g, 20 mmol), DMSO (17 mL), and NMP (17 mL) were added to another flask. After the monomers were dissolved, potassium carbonate (4.146 g, 30 mmol) was added. The same method used for the syntheses of the hydrophilic oligomers was used to remove the water and toluene in the flask. Then, the polymerization was allowed to proceed at 100°C for 5 h to prepare hydrophobic oligomers. The solution of hydrophilic oligomers, DMSO (20 mL) and NMP (50 mL), was added to the hydrophobic oligomer solution with a syringe. The bath temperature was raised to 140°C and maintained for 24 h. The reaction solution was poured into an excess of deionized water. The obtained polymer was then immersed in a 6 wt % HCl solution overnight to convert the polymer into an acid form. The excess acid was washed with water, and then the polymer was dried in a vacuum oven at 80°C for 24 h.

Membrane preparation

Membranes were prepared via the casting of 10 wt % polymer solutions in NMP onto glass plates. They were dried at 80°C for 12 h and at 100°C for another 48 h. The membranes were detached from the glass plates by immersion into deionized water. The membranes were

then stored in deionized water until use. The thickness of the wet membranes was about 100 μm .

Measurements

$^1\text{H-NMR}$ spectra were obtained on a Bruker Avance 500 NMR spectrometer (Yokohama, Japan). $\text{DMSO-}d_6$ was used as a solvent for the hydrophilic oligomers. The hydrophobic oligomers and the copolymers were measured in a mixture of $\text{DMSO-}d_6$ and $\text{NMP-}d_9$.

The molecular weights of the hydrophilic oligomers were measured with a gel permeation chromatography (GPC) system (LC-6A, Shimadzu, Kyoto, Japan) equipped with a size exclusion chromatography column (TSK-GEL α -5000, Tosoh, Tokyo, Japan) and a refractive-index detector (RID-10V, Shimadzu). DMSO was used as a mobile phase at 40°C. A calibration curve for the hydrophilic oligomers was prepared with molecular weight standards of poly(methyl methacrylate)s. The molecular weights of the hydrophobic oligomers and all the copolymers were measured with the GPC system equipped with an ultraviolet detector (SPD-6AV, Shimadzu). NMP was used as a mobile phase at 40°C. A calibration curve was prepared with molecular weight standards of polystyrene.

The surface morphology of the membranes was observed with an atomic force microscope (SPI3800N/SPA400, SII Co., Tokyo, Japan) in the tapping mode. Thin membranes were prepared via the spin coating of a 1 wt % polymer solution onto a silicon wafer at 3000 rpm for 60 s at room temperature.

The small-angle X-ray scattering (SAXS) of dry membranes was measured with a Nano-Viewer RA-Micro 7 (Rigaku Co., Tokyo, Japan). The measurements were made with a $\text{Cu K}\alpha$ radiation generator

(wavelength = 0.1542 nm) operating at 40 kV and 20 mA for 15 min at room temperature. The camera length was 85.5 mm. The scattering vector (\mathbf{q}) was defined as follows:

$$\mathbf{q} = \frac{4\pi}{\lambda} \sin \theta \quad (1)$$

where λ and 2θ are the wavelength of the X-rays and the scattering angle, respectively.

Thermogravimetric analysis (TGA) was carried out with a TGA-50 (Shimadzu). Samples were dried at 80°C to remove the water before TGA. They were then heated from room temperature to 700°C at a heating rate of 10°C/min under air flowing at 50 mL/min.

The IEC of the membranes was determined by a titration method.^{15,16} The water uptake was measured by a weight difference methodology. A wet membrane, which was soaked in deionized water for at least 24 h, was weighed, dried in a vacuum oven at 100°C for 24 h, and then weighed again. The following equation was used for the water uptake:

$$\text{Water uptake (\%)} = \frac{W_{\text{wet}} - W_{\text{dry}}}{W_{\text{dry}}} \times 100 \quad (2)$$

where W_{wet} is the weight of the wet membrane and W_{dry} is the weight of the dry membrane.

The states of the water in the membranes were evaluated with a PerkinElmer DSC-7 (Waltham, MA). The surface of a water-swollen membrane was wiped with Kimwipes paper, and a sample was weighed before it was sealed hermetically in an aluminum differential scanning calorimetry (DSC) pan. An empty pan with a lid was used as a reference. Samples were equilibrated at -50°C for 5 min and then heated at a ramp rate of 5°C/min up to 10°C with the standard DSC mode.

The proton conductivity of the membranes was measured by the ac impedance method at 25 and 50°C with a relative humidity of 90%. The conductivity [σ (S/cm)] of the samples in the longitudinal direction was calculated with the following equation:

$$\sigma = \frac{l}{RS} \quad (3)$$

where l is the distance between the electrodes used to measure the potential ($l = 1$ cm), R (Ω) is the impedance of the membrane, and S (cm^2) is the cross-sectional area of the membrane.

The methanol permeability was determined at room temperature (25°C) with a pair of glass chambers (each chamber was 20 mL in volume and had a cross section of 6.6 cm^2); there was water in one chamber, and there was a 1 mol/L methanol solution in the other chamber. A membrane was set between the two chambers. The methanol permeabil-

ity was obtained by periodic measurements of the methanol concentration in the water chamber with a gas chromatograph (GC-8A, Shimadzu). The methanol permeability through the membrane was determined as follows:¹⁷

$$P = DK = \frac{1}{S} \frac{C_B(t)}{C_A(t - t_0)} V_B L \quad (4)$$

where P is the methanol permeability (cm^2/s); S (cm^2) and L (cm) are the membrane area and thickness, respectively; C_A (mmol/L) is the concentration of the methanol in the methanol chamber; C_B (mmol/L) is the methanol concentration in water chamber B; V_B (mL) is the water volume in the water chamber; t is the permeation time (s); and t_0 is the time lag.¹⁷ D and K are the methanol diffusivity and partition coefficient between the membrane and the adjacent solution, respectively. DK is the permeability, which was evaluated from the slope of the linear line in a plot of C_B against t .

RESULTS AND DISCUSSION

Synthesis and characterization of the SPAES polymers

A series of random SPAES copolymers were successfully synthesized by the nucleophilic aromatic substitution polycondensation of SDFDPS, SHQK, DFDPS, and DHN with anhydrous potassium carbonate, as shown in Scheme 1. Copolymers with various IECs were prepared through the control of the ratio of sulfonated monomers (SDFDPS and SHQK) to nonsulfonated monomers (DFDPS and DHN). The molecular weights and IECs of the prepared random copolymers are summarized in Table I. Five kinds of random SPAES copolymers with different IECs (RC-1, RC-2, RC-3, RC-4, and RC-5) were prepared.

To synthesize multiblock copolymers, there are usually two approaches. In one approach, a terminal-activated oligomer is first synthesized. The oligomer is then copolymerized with other monomers to prepare multiblock copolymers.¹⁸ Another approach uses the reaction between different types

TABLE I
Molecular Weights and IECs of Random SPAES Copolymers

Polymer	M_n (kDa)	M_w (kDa)	IEC (mmol/g)
RC-1	30	200	0.77
RC-2	41	280	0.86
RC-3	67	170	1.56
RC-4	39	240	1.76
RC-5	54	120	2.27

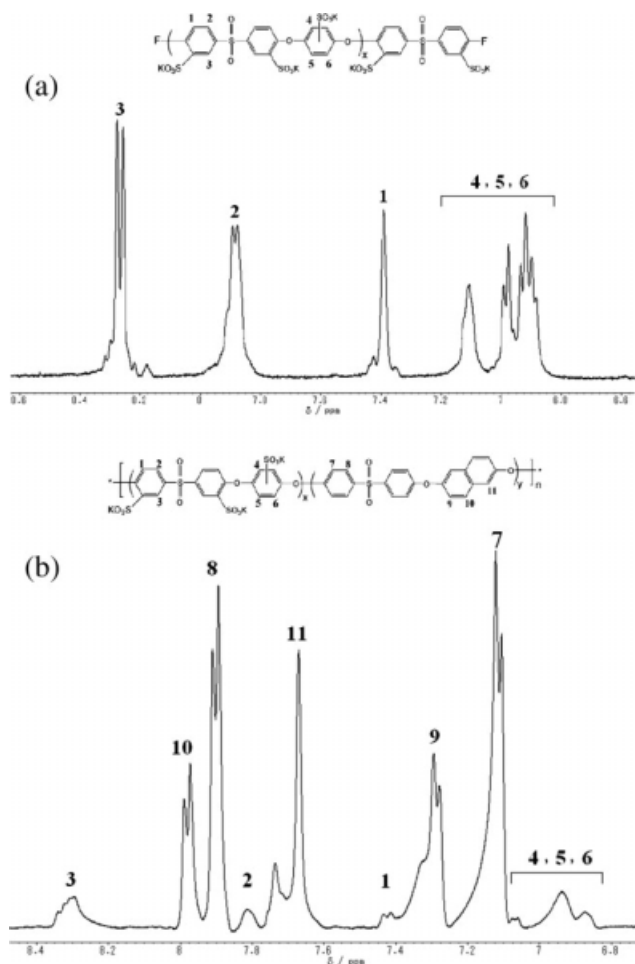


Figure 1 ¹H-NMR spectra of (a) a hydrophilic oligomer and (b) a multiblock polymer (MBC-3).

of terminal-activated oligomers.^{19,20} In this study, the multiblock copolymer was synthesized via the latter approach, as shown in Scheme 2. First, a fluorine-terminated hydrophilic oligomer (oligomer 1) was synthesized. The synthesized hydrophilic oligomer was confirmed by ¹H-NMR in DMSO-*d*₆, as shown in Figure 1(a). The number-average molecular weight (M_n) and weight-average molecular weight (M_w) of the hydrophilic oligomer were 27,000 and 85,000, respectively. The hydrophobic oligomer (oligomer 2) was synthesized by the reaction of DFDPS and DHN. Through control of the initial monomer ratios, several different hydrophobic oligomers with M_w values ranging from 5000 to 80,000 were prepared. Multiblock copolymers were obtained by the reaction of hydrophilic oligomer 1 with hydrophobic oligomer 2. The ¹H-NMR spectrum of a typical multiblock copolymer is shown in Figure 1(b). All the chemical shifts of protons were assigned to the protons of the supposed chemical structure of the multiblock copolymers. Three kinds of multiblock copolymers with different IECs (MBC-1, MBC-2, and

TABLE II
Molecular Weights and IECs of Multiblock SPAES Copolymers

Polymer	M_n (kDa)	M_w (kDa)	IEC (mmol/g)
MBC-1	39	230	0.58
MBC-2	52	170	1.22
MBC-3	69	190	1.77

MBC-3) were synthesized. Their molecular weights and IECs are summarized in Table II.

Morphology of the SPAES membranes

The morphology of a PEM generally plays an important role in its performance in fuel cell applications.²¹ Microstructures can influence the properties of membranes, especially the spatial distribution of ionic sites.²² Nafion membrane is very famous for its hydrophilic and hydrophobic phase-separated structure, which makes it possible for it to have a high proton conductivity even with a low IEC.²³ To evaluate the phase-separated structures in our SPAES copolymers, we carried out atomic force microscopy (AFM) and SAXS measurements.

The surface morphologies of the spin-coated polymers on random RC-2, random RC-4, multiblock MBC-3, and Nafion were observed by AFM in the tapping mode at 60% relative humidity, as shown in Figure 2. The dark regions in the images, which

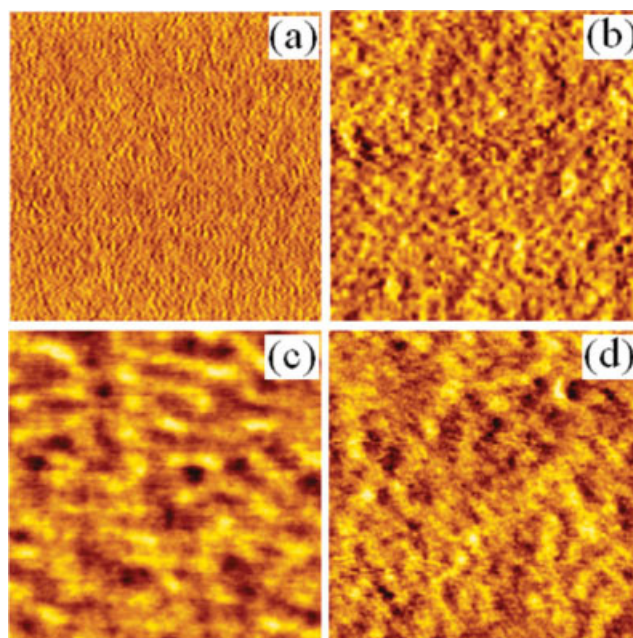


Figure 2 AFM phase images of spin-coated polymers at room temperature with a relative humidity of 60% (scan size = 500 nm × 500 nm): (a) random SPAES RC-2, (b) random SPAES RC-4, (c) multiblock SPAES MBC-3, and (d) Nafion. [Color figure can be viewed in the online issue, which is available at www.interscience.wiley.com.]

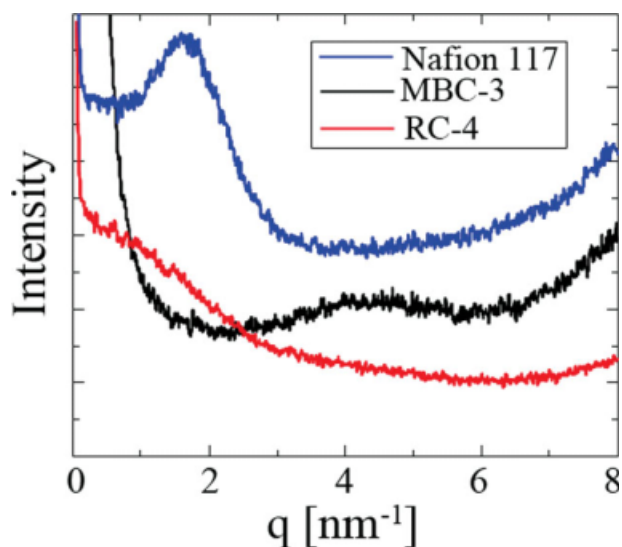


Figure 3 SAXS profiles of Nafion 117, random SPAES RC-4, and multiblock SPAES MBC-3 at 25°C. [Color figure can be viewed in the online issue, which is available at www.interscience.wiley.com.]

were assigned to softer regions, represent the hydrophilic parts of the membrane, whereas the bright regions were assigned to the hydrophobic parts.^{24,25} The size and connection of these two regions are supposed to have a great influence on the proton and methanol transport properties through the membranes.²⁶ For random SPAES membranes [RC-2; Fig. 2(a)], the dark regions (considered to be the hydrophilic parts) were less aggregated and randomly distributed in the polymer matrix. The IEC increase led to larger domains of bright and dark regions [RC-4; Fig. 2(b)]; however, the phase separation was not clear yet. On the other hand, a multiblock SPAES membrane [MBC-3; Fig. 2(c)] had a clearly phase-separated structure and larger dark regions; this was similar to the morphology of the Nafion membrane [Fig. 2(d)]. This might be because the long hydrophilic and hydrophobic units in the multiblock copolymers developed phase separation.²⁷ This phase-separated structure is expected to be beneficial for keeping water in the membrane and for forming proton transport channels.

The AFM measurements provided information about the surfaces of the membranes. SAXS measurements were useful in investigating the bulk morphology of the membranes.^{28,29} The SAXS profiles of the random RC-4 membrane, multiblock MBC-3 membrane, and Nafion 117 in their dry forms are shown in Figure 3. We observed intensity peaks at q values of approximately 1.64 and 4.30 nm^{-1} for the Nafion 117 and multiblock MBC-3 membranes, respectively. These peaks were supposed to be caused by the clustering of the ionic groups in the polymer matrix.^{28,29} The Bragg spacing (d), which

refers to the center-to-center distance between two ionic clusters, indicated the size of the ionic clusters in the membranes. d could be calculated as follows: $d = 2\pi/q$.³⁰ The center-to-center distances of the Nafion 117 and multiblock MBC-3 membranes were determined to be 3.8 and 1.5 nm, respectively. For the random RC-4 membrane, no obvious peak was observed. These SAXS investigations suggested that the multiblock MBC-3 membrane had nanoscale clusters.

Thermal stability of the membranes

The thermal stability of the membranes was evaluated by TGA. Figure 4 shows the TGA curves of the membranes prepared from the RC-4 random copolymer, MBC-3 multiblock copolymer, and Nafion 117. For the random and multiblock SPAES membranes, two regions of thermal decomposition were observed. The first weight loss (300–400°C) was attributed to the decomposition of sulfonic acid groups, and the second weight loss corresponded to the decomposition of the main chain of the copolymers.³¹ Although there was a small difference in the TGA profiles between the random RC-4 and multiblock MBC-3 membranes, both kinds of copolymers had good thermal stability, up to approximately 300°C, which was comparable to that of the Nafion 117 membrane.

Water uptake of the membranes and water states in the membranes

In general, proton and methanol transport behaviors strongly depend on the IEC and water uptake of a membrane and on the water state in a

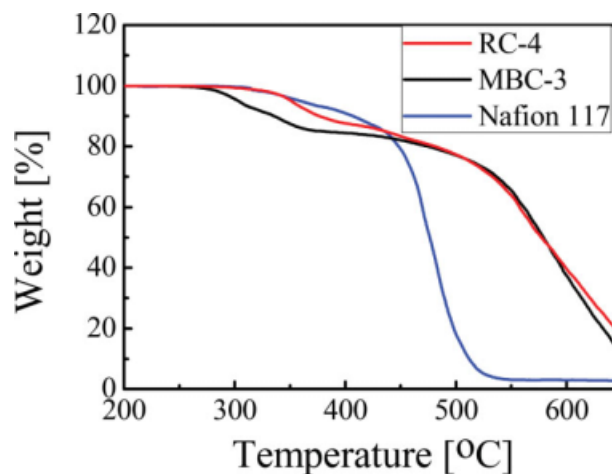


Figure 4 TGA curves of random SPAES RC-4, multiblock SPAES MBC-3, and Nafion 117. [Color figure can be viewed in the online issue, which is available at www.interscience.wiley.com.]

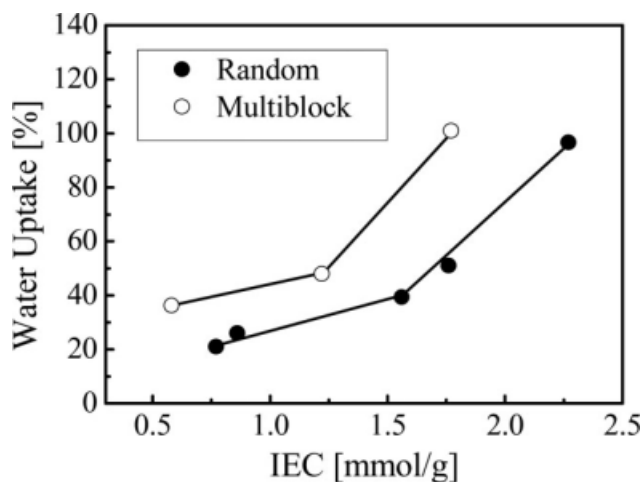


Figure 5 Effect of the IEC on the water uptake of random and multiblock SPAES membranes at room temperature.

membrane.^{32,33} Figure 5 shows the water uptake of the random and multiblock SPAES membranes as a function of the IEC. The water uptake of the two series of membranes increased with an increase in the IEC because the sulfonic acid groups would hold water in the membranes. At similar IECs, the water uptake of the multiblock SPAES membranes was higher than that of the random SPAES membranes. For random SPAES copolymers, the sulfonic acid groups would be randomly distributed in the copolymer chain.³⁴ Unlike random SPAES copolymers, the multiblock SPAES copolymers had repeated hydrophilic and hydrophobic units. These (repeated units) were thought to be able to assemble into clusterlike structures or spherical or cylindrical micelles,²⁵ as also confirmed by our AFM and SAXS measurements. These kinds of structures made the hydrophilic domains well connected and tended to effectively keep more water in the membranes.

Water in a PEM is usually classified into three types.^{35–37} The first is nonfreezing bound water, which strongly binds to a polymer chain. The second is freezing bound water, which weakly binds to a polymer chain and interacts weakly with the non-freezing bound water. The third is free water, which does not bind to a polymer but behaves as bulk water. The states of the water in a membrane greatly affect the membrane's performance. It has been reported that a low fraction of free water in membranes generally leads to a low electro-osmotic drag during fuel cell operation, resulting in low methanol permeabilities.³⁸ Figure 6 shows the DSC melting curves of the random RC-4 and RC-5 membranes and the multiblock MBC-3 membrane. The random RC-4 membrane and multiblock MBC-3 membrane had similar IECs. The RC-5 membrane and MBC-3 membrane had almost the same water uptake. In these DSC measurements, two neighboring melting

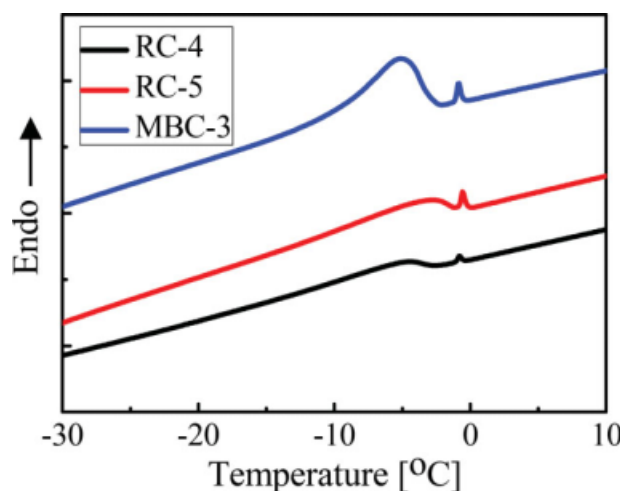


Figure 6 DSC melting curves of random and multiblock SPAES membranes. [Color figure can be viewed in the online issue, which is available at www.interscience.wiley.com.]

peaks were observed. Upon heating, the first broad peak was observed below 0°C, and it belonged to the freezing bound water.³⁷ The second sharp peak, which was observed near 0°C, was derived from the free water. Because these two peaks usually overlap each other, in this study, we classified the sum of the free water and freezing bound water as freezable water. The amount of freezable water could be calculated from the ratio of the endothermic peak areas to the heat of fusion (334 J/g) for pure water.¹⁷ The bound water was calculated from the difference between the total water content and freezable water content because bound water cannot be detected by DSC. The freezable and bound water contents are summarized in Table III. When we compared RC-4 and RC-5, the increase in the IEC resulted in an increase in both the freezable water and bound water contents. Bound water usually binds with a sulfonic acid group in a membrane.¹⁷ With the increase in the IEC, there were more sulfonic acid groups in the membrane, and this allowed it to keep more bound water. In addition, the higher IEC

TABLE III
Freezable Water Contents and Bound Water Contents of Random and Multiblock SPAES Membranes Based on DSC Measurements

	IEC (mmol/g)	Water content (%)	Freezable water content (%)	Bound water content (%)
Random				
RC-4	1.76	33.8	6.8	27.0
RC-5	2.27	49.1	12.3	36.8
Multiblock				
MBC-3	1.77	50.2	22.7	27.5

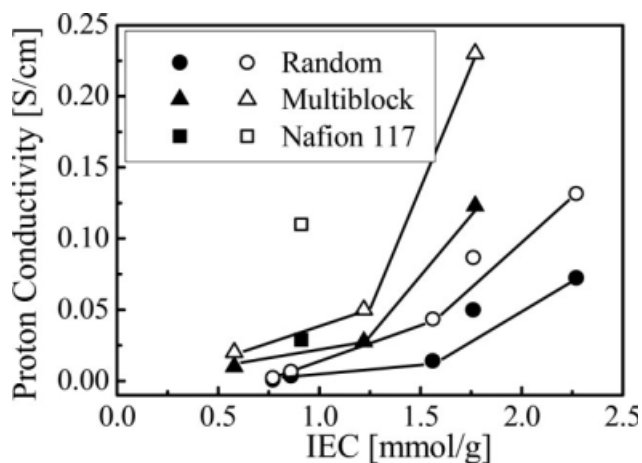


Figure 7 Proton conductivity of random SPAES, multiblock SPAES, and Nafion 117 at (●,▲,■) 25 and (○,△,□) 50°C.

possibly improved the continuity of the hydrophilic parts in a membrane,³⁹ which could significantly increase the water content of the membrane. When we compared the random RC-4 membrane and multiblock MBC-3 membrane, which had almost the same IEC, the bound water contents of the two membranes were almost the same. Interestingly, the freezable water content of the multiblock MBC-3 membrane was much higher than that of the random RC-4 membrane. This could be attributed to the ionic clusters that formed in the multiblock copolymer because the freezable water is likely to exist around bound water and in the ionic clusters of a polymer network.⁴⁰

Proton conductivity of the membranes

The proton conductivity of the SPAES membranes was measured at 25 and 50°C with 90% relative humidity, as shown in Figure 7. The proton conductivity of the Nafion 117 membrane is also plotted in this figure. For random and multiblock SPAES membranes, the proton conductivity increased with increases in the IEC and temperature. This increase in the proton conductivity can be explained by an increase in the sulfonic acid contents of the membranes and by the subsequent increase in the water uptake.

Multiblock SPAES membranes showed higher proton conductivity values than random SPAES membranes at the same IEC, and this was similar to the results for water uptake. The proton conductivity of sulfonated polymers depends on the type of charge carrier and on the carrier mobility. Moreover, the mobility is mainly ensured by the presence of water molecules and their clusters. The proton conductivity through a PEM is known to occur via two

routes.⁴¹ One is the hopping or jumping (Grotthuss) mechanism, in which a proton passes along fixed sulfonic acid sites and a chain of water molecules. The other is the vehicle mechanism, in which a proton combines with a solvent molecule, yielding a complex such as H_3O^+ , and this complex is transported through a membrane. In both of these mechanisms, a continuous water network and mobile freezable water are essential because they provide the pathway for the protons or vehicles to transport the protons. The SAXS and DSC results suggested that the multiblock SPAES copolymer had ionic clusters and could keep a considerable amount of freezable water in the SPAES membrane, which led to effective proton transport.

Methanol permeability of the membranes and proton/methanol selectivity in the permeation

The methanol permeability of a PEM is another significant property for the application of a DMFC. High methanol permeation results not only in low fuel efficiency but also in low overall voltage performance. Thus, it is very important to develop a PEM with low methanol permeability. The methanol permeabilities of the SPAES membranes as a function of the IEC are shown in Figure 8. The methanol permeabilities of all of the SPAES membranes were lower than that of the Nafion 117 membrane. Like the proton conductivity, the methanol permeability increased with an increase in the IEC. The higher IECs of the copolymers meant higher water contents and a higher amount of the hydrophilic moiety in the membranes. The high water content and high amount of the hydrophilic moiety mediated not only the proton transport but also the methanol transport through the membrane. When the multiblock and

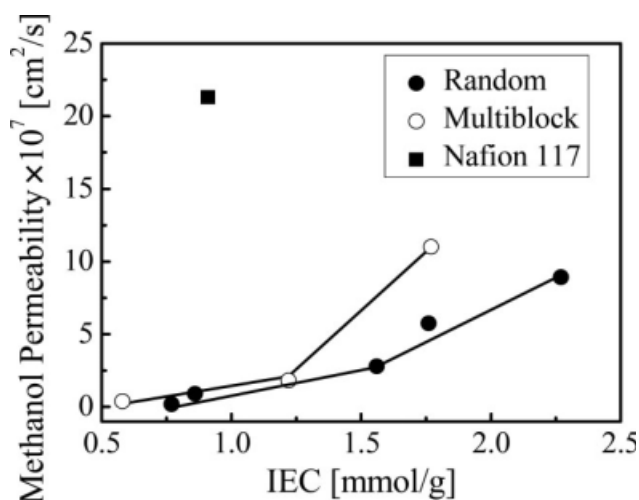


Figure 8 Methanol permeability of random SPAES, multiblock SPAES, and Nafion 117 at 25°C.

random copolymers had similar IECs, the multiblock SPAES membrane showed slightly higher methanol permeability. This was related to the higher water uptake and to the ionic clusters that formed in the multiblock membrane.

Recently, there have been numerous reports of PEMs with low methanol permeability. Cho et al.⁴² reported a poly(styrene-*b*-vinyl benzyl phosphonic acid)/poly(2,6-dimethyl-1,4-phenylene oxide) blend membrane with a methanol permeability of $5.3 \times 10^{-9} \text{ cm}^2/\text{s}$. Fei et al.⁴³ synthesized inorganic-organic hybrid polymers with pendent sulfonated cyclic phosphazene side groups as proton-conductive materials and found that the average methanol permeability was around $10^{-9} \text{ cm}^2/\text{s}$. However, the proton conductivities of these membranes were also low, with values of 5.38×10^{-4} and $1.13 \times 10^{-4} \text{ S/cm}$ (at 25°C), respectively.

Proton/methanol selectivity is defined as the ratio of the proton conductivity to the methanol permeability. This selectivity is a useful way of evaluating PEMs because an ideal PEM for a DMFC is expected to have high proton conductivity and low methanol permeability.⁴⁴ Figure 9 shows the proton conductivity of the SPAES membranes (at 25°C and 90% relative humidity) as a function of the methanol permeability. The slopes of the solid lines correspond to the selectivities of the membranes. Both the random and multiblock SPAES membranes showed higher proton/methanol selectivity than the Nafion 117 membrane. To compare these SPAES membranes with other PEMs reported in the literature, we summarized the proton/methanol selectivities of the membranes in Figure 10. The multiblock membranes showed quite high selectivities. In particular, because of the low methanol permeability, the MBC-1 membrane exhibited the highest selectivity among these membranes.

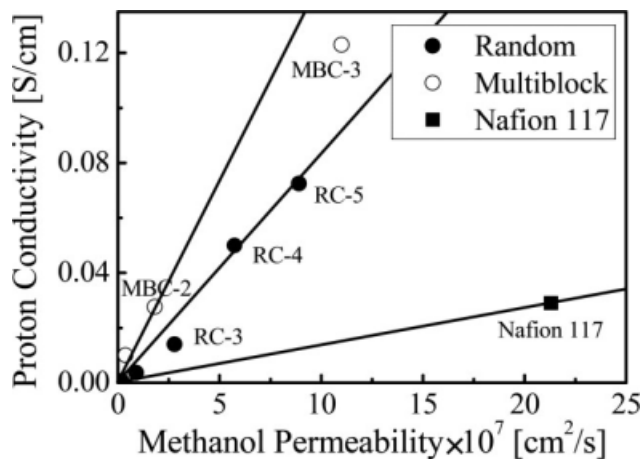


Figure 9 Proton conductivity of random SPAES, multiblock SPAES, and Nafion 117 as a function of methanol permeability (at 25°C).

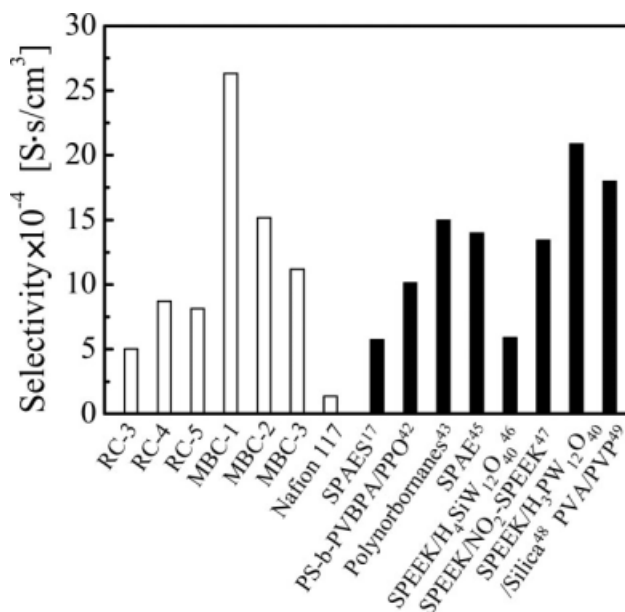


Figure 10 Proton/methanol selectivity of SPAES membranes and other kinds of reported membranes.^{17,42,43,45-49} PPO = poly(2,6-dimethyl-1,4-phenylene oxide); PS-*b*-PVBPA = poly(styrene-*b*-vinyl benzyl phosphonic acid); SPAE = sulfonated poly(arylene ether); PVA = poly(vinyl alcohol); PVP = polyvinylpyrrolidone.

Most PEMs with high proton conductivity are highly permeable to methanol molecules.⁵⁰ Qi et al.⁵¹ synthesized benzimidazole-containing sulfonated poly(ether sulfone)s with high proton conductivity for fuel cell applications. The proton conductivity of one of their membranes was 0.12 S/cm at room temperature with a relative humidity of 100%. However, the methanol permeability of the membranes was not reported. Our MBC-3 membrane also showed proton conductivity of 0.12 S/cm (at 25°C and 90% relative humidity) and with relatively high methanol permeability ($1.1 \times 10^{-6} \text{ cm}^2/\text{s}$ at 25°C). Fu et al.⁵² reported SPEEK/epoxy/phenol novolac blend PEMs, one of which showed low methanol permeability of $3.6 \times 10^{-8} \text{ cm}^2/\text{s}$ and proton conductivity of approximately 0.01 S/cm with 100% relative humidity at 20°C . Our MBC-1 membrane exhibited a performance (methanol permeability of $3.6 \times 10^{-8} \text{ cm}^2/\text{s}$ and proton conductivity of 0.01 S/cm at 90% relative humidity and 25°C) almost comparable to the performance of this membrane. In a word, for a DMFC application, the optimum PEM should have the lowest methanol permeability and the highest proton conductivity; however, many studies on PEMs have shown that a decrease in the methanol permeability comes with a decrease in the proton conductivity. Thus, a compromise between the two properties has to be reached to design desirable PEMs.

CONCLUSIONS

Random and multiblock copolymers of SPAES were synthesized and evaluated as possible materials for the PEM of a DMFC. The water uptake, proton conductivity, and methanol permeability values of the SPAES membranes depended on the contents of the sulfonate group in the membranes. Multiblock SPAES membranes exhibited higher water uptake and proton conductivity values than random SPAES membranes. AFM observations and SAXS measurements suggested that the high values could be due to the microphase separation and ionic clusters of the multiblock SPAES membranes. Like other copolymers reported, block SPAES copolymers have a high potential for use as PEMs because of their high proton conductivities and low methanol permeabilities.

The authors thank Atsunori Mori at Kobe University for his help with the $^1\text{H-NMR}$ analyses. This study was partly supported by Special Coordination Funds for Promoting Science and Technology, Creation of Innovation Centers for Advanced Interdisciplinary Research Area (Innovation Bio-production Kobe), MEXT, Japan.

References

- Arico, A. S.; Creti, P.; Antonucci, P. L.; Cho, J.; Kim, H.; Antonucci, V. *Electrochim Acta* 1998, 43, 3719.
- Ishikawa, J.-I.; Fujiyama, S.; Inoue, K.; Omi, T.; Tamai, S. *J Membr Sci* 2007, 298, 48.
- Zhang, F.; Li, N.; Cui, Z.; Zhang, S.; Li, S. *J Membr Sci* 2008, 314, 24.
- Park, Y.-S.; Yamazaki, Y. *Solid State Ionics* 2005, 176, 1079.
- Chikashige, Y.; Chikyu, Y.; Miyatake, K.; Watanabe, M. *Macromol Chem Phys* 2006, 207, 1334.
- Lin, C. W.; Fan, K. C.; Thangamuthu, R. *J Membr Sci* 2006, 278, 437.
- Karlsson, L. E.; Jannasch, P. *J Membr Sci* 2004, 230, 61.
- Wang, F.; Hickner, M.; Kim, Y. S.; Zawodzinski, T. A.; McGrath, J. E. *J Membr Sci* 2002, 197, 231.
- Gil, M.; Ji, X.; Li, X.; Na, H.; Hampsey, J. E.; Lu, Y. *J Membr Sci* 2004, 234, 75.
- Li, Q.; He, R.; Jensen, J. O.; Bjerrum, N. J. *Fuel Cells* 2004, 4, 147.
- Zhang, X.; Liu, S.; Yin, J. *J Membr Sci* 2005, 258, 78.
- Zhao, C.; Li, X.; Wang, Z.; Dou, Z.; Zhong, S.; Na, H. *J Membr Sci* 2006, 280, 643.
- Roy, A.; Hickner, M. A.; Yu, X.; Li, Y.; Glass, T. E.; McGrath, J. E. *J Polym Sci Part B: Polym Phys* 2006, 44, 2226.
- Onodera, T.; Sasaki, M.; Yamiki, D. *Jpn. Pat.* 139,432A (2005).
- Brijmohan, S. B.; Swier, S.; Weiss, R. A.; Shaw, M. T. *Ind Eng Chem Res* 2005, 44, 8039.
- Chen, N.-P.; Hong, L. *Eur Polym J* 2001, 37, 1027.
- Kim, D. S.; Shin, K. H.; Park, H. B.; Chung, Y. S.; Nam, S. Y.; Lee, Y. M. *J Membr Sci* 2006, 278, 428.
- Genies, C.; Mercier, R.; Sillion, B.; Cornet, N.; Gebel, G.; Pineri, M. *Polymer* 2001, 42, 359.
- Shibata, M.; Cao, J.; Yosomiya, R. *Polymer* 1997, 38, 3103.
- Ghassemi, H.; Ndip, G.; McGrath, J. E. *Polymer* 2004, 45, 5855.
- Yang, Y. S.; Shi, Z. Q.; Holdcroft, S. *Macromolecules* 2004, 37, 1678.
- Gouin, J. P.; Williams, C. E.; Eisengerg, A. *Macromolecules* 1989, 22, 4573.
- Fujimura, M.; Hashimoto, T. J.; Kawai, H. *Macromolecules* 1981, 14, 1309.
- Storey, R. F.; Baugh, D. W. *Polymer* 2000, 41, 3205.
- Ghassemi, H.; McGrath, J. E.; Zawodzinski, T. A. *Polymer* 2006, 47, 4132.
- Li, Z.; Zhang, G.; Xu, D.; Zhao, C.; Na, H. *J Power Sources* 2007, 165, 701.
- Won, J.; Park, H. H.; Kim, Y. J.; Choi, S. W.; Ha, H. Y.; Oh, I.-H.; Kim, H. S.; Kang, Y. S.; Ihn, K. J. *Macromolecules* 2003, 36, 3228.
- Yang, B.; Manthiram, A. *J Power Sources* 2006, 153, 29.
- Takimoto, N.; Wu, L.; Ohira, A.; Takeoka, Y.; Rikukawa, M. *Polymer* 2009, 50, 534.
- Lu, X.; Steckle, W. P.; Weiss, R. A. *Macromolecules* 1993, 26, 6525.
- Bae, B.; Miyatake, K.; Watanabe, M. *J Membr Sci* 2008, 310, 110.
- Jiang, R.-C.; Kunz, H. R.; Fenton, J. M. *J Membr Sci* 2006, 272, 116.
- Park, H. B.; Lee, C. H.; Lee, Y. M.; Freeman, B. D.; Kim, H. J. *J Membr Sci* 2006, 285, 432.
- Li, Y.; Roy, A.; Badami, A. S.; Hill, M.; Yang, J.; Dunn, S.; McGrath, J. E. *J Power Sources* 2007, 172, 30.
- Tasaka, M.; Suzuki, S.; Ogawa, Y. *J Membr Sci* 1988, 38, 175.
- Ping, Z. H.; Nguyen, Q. T.; Chen, S. M.; Zhou, J. Q.; Ding, Y. D. *Polymer* 2001, 42, 8461.
- Jung, B. S.; Kim, B. Y.; Yang, J. M. *J Membr Sci* 2004, 245, 61.
- Ise, M.; Kreuer, K. D.; Maier, J. *Solid State Ionics* 1999, 125, 213.
- Kim, Y. S.; Hickner, M. A.; Dong, L.; Pivovar, B. S.; McGrath, J. E. *J Membr Sci* 2004, 243, 317.
- Qu, X.; Wirsén, A.; Albertsson, A.-C. *Polymer* 2000, 41, 4589.
- Pivovar, B. S.; Wang, Y.-X.; Cussler, E. L. *J Membr Sci* 1999, 154, 155.
- Cho, C. G.; Kim, S. H.; Park, Y. C.; Kim, H.; Park, J.-W. *J Membr Sci* 2008, 308, 96.
- Fei, S.-T.; Wood, R. M.; Lee, D. W.; Stone, D. A.; Chang, H.-L.; Allcock, H. R. *J Membr Sci* 2008, 320, 206.
- Robeson, L. M. *J Membr Sci* 1991, 62, 165.
- Kim, D. S.; Robertson, G. P.; Guiver, M. D.; Lee, Y. M. *J Membr Sci* 2006, 281, 111.
- Ismail, A. F.; Othman, N. H.; Mustafa, A. *J Membr Sci* 2009, 329, 18.
- Lin, C.-K.; Kuo, J.-F.; Chen, C.-Y. *J Power Sources* 2009, 187, 341.
- Bello, M.; Zaidi, J.; Rahman, S. U. *J Membr Sci* 2008, 322, 218.
- Huang, Y. F.; Chuang, L. C.; Kannan, A. M.; Lin, C. W. *J Power Sources* 2009, 186, 22.
- Hong, Y. T.; Lee, C. H.; Park, H. S.; Min, K. A.; Kim, H. J.; Nam, S. Y.; Lee, Y. M. *J Power Sources* 2008, 175, 724.
- Qi, Y.; Gao, Y.; Tian, S.; Hill, A. R.; Gaudet, J.; Guay, D.; Hay, A. S. *J Polym Sci Part A: Polym Chem* 2009, 47, 1920.
- Fu, T.; Zhong, S.; Cui, Z.; Zhao, C.; Shi, Y.; Yu, W.; Na, H.; Xing, W. *J Appl Polym Sci* 2009, 11, 1335.